INTERACTION OF NANOSECOND LASER PULSES WITH BIOLOGICAL TISSUE PHANTOMS

Emil-Alexandru BRUJAN

Department of Hydraulics, University Politehnica, Spl. Independentei 313, 060042 Bucharest, Romania
E-mail: eabrujan@yahoo.com

Shock wave emission and cavitation bubble dynamics after optical breakdown in water and elastic-plastic media with Nd:YAG laser pulses of 6-ns duration is investigated experimentally. The elastic-plastic media consist of a polyacrylamide (PAA) gels whose elastic properties can be controlled by modifying the water content of the sample. Scaling laws for the maximum amplitude of the shock wave emitted during optical breakdown and bubble collapse as well as maximum bubble radius are presented.

Key words: elastic-plastic media; optical beakdown; shock waves; cavitation.

1. INTRODUCTION

In the last years, the interaction of laser light with biological tissue have been the object of extensive research [1-6]. This interest was motivated by the increasingly important role of cavitation and associated bubble dynamics in medical applications. However, an important consideration that has only recently received much attention is the role of the mechanical properties of biological tissue on the shock wave emission during optical breakdown and cavitation. The currently understanding of these processes in the body originates from studies of bubble dynamics in Newtonian liquids (mainly water). The nearly ubiquitous elastic-plastic behaviour of biological tissues may have a profound influence on the shock wave emission and cavitation bubbles dynamics. Thus, a characterization of these effects in media with mechanical properties similar to that of biological tissues is of interest for an optimization of the surgical procedures.

2. EXPERIMENTAL

The bubbles were generated by using a Q-switched Nd:YAG laser (Continuum YG 671-10) which delivers light pulses at a wavelength of 1064 nm with energies of up to 250 mJ and a pulse duration of 6 ns. The elastic-plastic media consist of a polyacrylamide (PAA) gels whose elastic properties can be controlled by modifying the water content of the sample. The PAA sample was mounted in a teflon holder and completely immersed in water during experiments. Achromats were used for beam collimation and focusing to minimize spherical aberrations, and for the same purpose an ophthalmic contact lens corrected for an air water transition (Rodenstock RYM) was built into the cuvette wall [7]. The dynamics of the cavitation bubble was recorded with a high-speed image converter camera (Hadland Photonics, Imacon 792) using a slow scan CCD camera system (Photometrics AT200A) with a 1317 x 1035 pixel array. During each laser exposure, the pulse energy was measured using a pyroelectric energy meter (Laser Precision Rj 7100). The pulse-to-pulse fluctuations of the laser energy were in the range of ±3%. The pressure of the shock wave emitted during optical breakdown and first bubble collapse was measured using a PVDF hydrophone (Ceram) with a rise time of 12 ns, an active area of 1 mm^2, and a sensitivity of 21 mV/MPa.

The elastic-plastic media consisted of transparent gels of polyacrylmide (PAA) with a water content of 95%, 85%, 80%, and 70%, respectively. For 70% water content, 60 grams acrylamid and 1.6 grams bis-

acrylamide were mixed with 140 grams of 0.22 M aqueous Tris buffer (pH 9.5) and 1 ml 10% amoniumpersulfate (APS). The solution was then placed in a plastic container and mixed with 0.2 ml N,N,N',N'-tetramethylethylenediamine (TEMED) to initiate polymerisation. For higher water content, the stock solution was diluted with buffer. The volume of each PAA sample was 20 x 15 x 15 mm^3. The elastic properties of the PAA samples were quantified by determining the stress-strain relation and calculating the elastic modulus, E, as the slope of the stress-strain curve. Uniaxial compression tests were performed on three specimens of PAA samples at each water content. The specimens were strained at a rate of $\dot{\varepsilon} = 1.7 \times 10^{-3}$ s^{-1} using a universal testing machine (Zwick 1456). The elastic modulus of the PAA samples was determined at 10% strain, with a standard deviation in E smaller than 7%. The yield strength of the samples was estimated by calculating the impact pressure generated by a high-speed liquid jet that penetrates the PAA sample. The jet is generated during the collapse of a cavitation bubble near the PAA sample and depending on the relative distance between bubble and PAA sample the jet has different impact velocities [7,8]. The water hammer pressure of a jet with a flat tip is $p_{WH} = \rho_1 c_1 \rho_2 c_2 v / (\rho_1 c_1 + \rho_2 c_2)$, where ρ_1, c_1 and ρ_2, c_2 are the respective densities and sound velocities in the jet and the impacted material, and v is the jet velocity [9]. The adopted value of the yield strength of the material corresponds to the lowest jet velocity for which a penetration into the PAA sample was observed. It should be noted here that this is only a low estimate of the yield strength of the material since the impact pressure can be up to three times higher when the jet tip is round or conical [10]. The measured values of the elastic modulus, density, sound velocity as well as an estimation of the yield strength of the PAA samples as a function of water content are given in Table 1.

Table 1. Physical properties of the PAA samples.

sample	water	PAA-95% water	PAA-85% water	PAA-80% water	PAA-70% water
E (MPa)	-	0.017 ± 0.001	0.124 ± 0.004	0.3 ± 0.01	0.4 ± 0.01
Y_0 (MPa)	-	-	20	60	80
ρ (kg/m^3)	998	1012 ± 10	1032 ± 10	1050 ± 10	1073 ± 10
c_0 (m/s)	1483	1518 ± 15	1560 ± 15	1575 ± 15	1605 ± 15

3. RESULTS AND DISCUSSION

The maximum pressure amplitude of the shock wave emitted during optical breakdown as a function of laser pulse energy is shown in Figure 1. The pressure values refer to a distance r of 10 mm between the laser focus and the site of measurement, where the portion of the shock wave intersecting the active area of the hydrophone can be approximated by a plane wave. In this and all following figures, each data point represents the averaged value of 8 measurements in the case of water and 6 measurements for the PAA samples. A first qualitative comment is that the shock wave amplitude increases with increasing the laser pulse energy E_L. For example, the maximum shock wave pressure in water is 0.7 MPa for $E_L = 1$ mJ and 2.64 MPa for $E_L = 10$ mJ. The corresponding values in the PAA sample with 70% water content are 0.5 MPa and 3 MPa, respectively. We further note that, independent of the water content of the sample, the maximum pressure amplitude of the shock waves is almost proportional to $E_L^{1/2}$. A proportionality $p \propto E_L^{1/2}$ was also determined by Schoeffman et al. [11] for laser-induced optical breakdown in water. A deviation from this scaling law is observed however for laser pulse energies smaller than 1 mJ and water content of the samples smaller than 80%.

In Figure 2, the maximal bubble radius is plotted as a function of the laser pulse energy. At equal laser pulse energy, the maximum radius of the cavitation bubble decreases with the water content of the sample and laser pulse energy. For example, in water the maximum bubble radius is 0.66 mm at 1 mJ and increases to 1.66 mm at an energy of 10mJ. In the PAA sample with 70% water content, the corresponding values are 0.46 mm and 1.13 mm, respectively. The scaling law for the size of the bubble oscillating in the PAA samples is the same as that in water, namely, the maximum bubble radius is proportional to the cube root of the laser pulse energy. This scaling law applies, however, only to laser pulse energies larger than 2 mJ, well above the breakdown threshold. For lower values, the energy dependence of the bubble size is stronger. A proportionality $R_{\max} \propto E_L^{1/3}$ was also determined by Vogel et al. [12] for a 6 ns laser-induced cavitation bubbles in water.
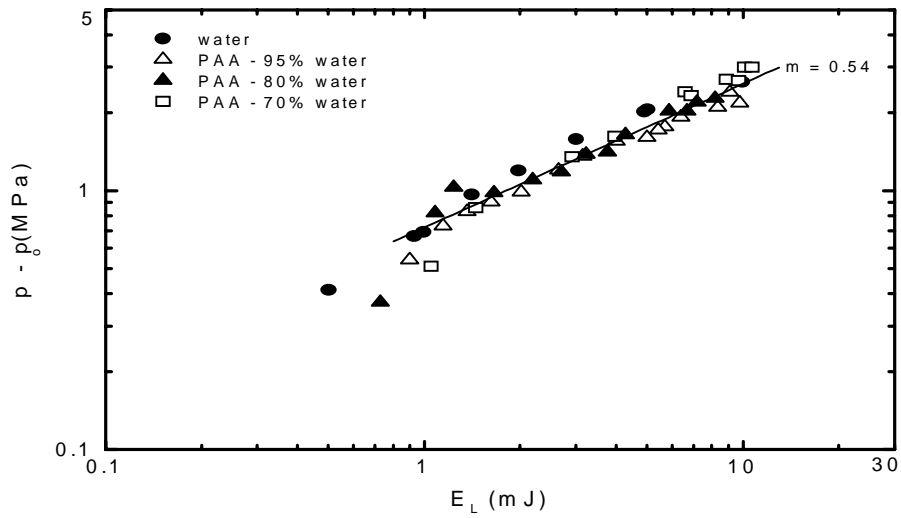
Fig.1 - Maximum amplitude of the shock wave emitted during optical breakdown, p, as a function of the laser pulse energy, E_L. The values are measured at a distance of 10 mm from the laser focus. The scaling law between the two parameters is $p \propto E_L^{1/2}$.
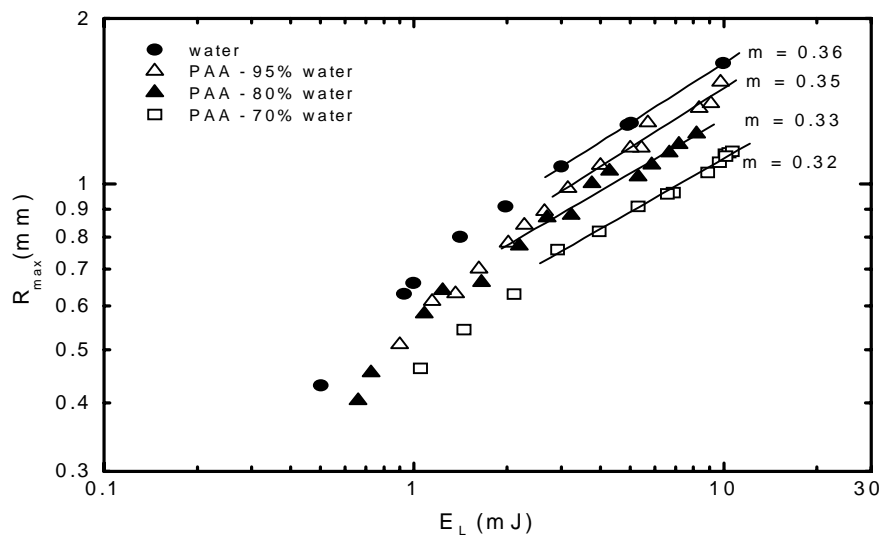
Fig.2 - Maximal cavitation bubble radius, R_{max}, as a function of the laser pulse energy, E_L. The slope of the straight lines gives the scaling law for the bubble radius at energy values well above the breakdown threshold. The same scaling law applies in water and PAA samples: $R_{max} \propto E_L^{1/3}$.
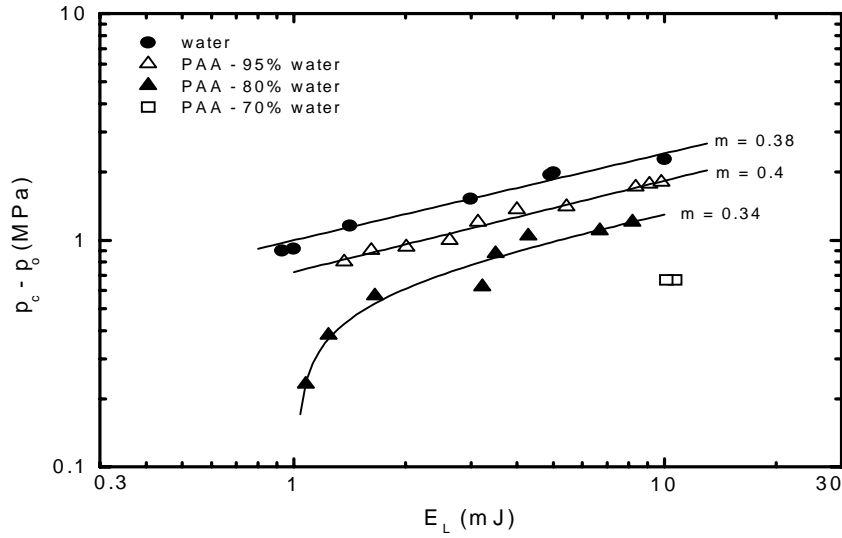
Fig. 3 - Maximum amplitude of the shock wave emitted during first bubble collapse as a function of the laser pulse energy. The values are measured at a distance of 10 mm from the laser focus. For energies well above the threshold the scaling law between maximum shock wave pressure during first bubble collapse and laser pulse energy is $p_c \propto E_L^{1/3}$. For the PAA sample with 80% water content there is a critical value of E_L below which no pressure pulse is generated during first bubble collapse.

In the same manner as for the initial transient pressure wave, we have examined the amplitude of the transient wave emitted during the first bubble collapse as a function of the laser pulse energy (Figure 3). In water and PAA sample with 95% water content, the measured values are fitted by a curve $(p_c - p_0) = aE_L^n$, with $a = 1$ and $n = 0.38$ for water, and $a = 0.73$ and $n = 0.4$ for the PAA sample with 95% water content; *i.e.* the pressure amplitude of this acoustic transient increases approximately proportional to the cube root of the laser pulse energy. For the PAA sample with 80% water content, the measured values are fitted by a curve $(p_c - p_0) = a(E_L - E_{L,c})^n$, with $a = 0.61$, $n = 0.34$, and $E_{L,c} = 1.01$ mJ. $E_{L,c}$ can be interpreted as a critical value of the laser pulse energy which determines the behaviour of the bubble: for $E_L \leq E_{L,c}$ the bubble dynamics is characterized by an overdamped behaviour where the maximum bubble radius is smoothly decreasing with the lapse of the time towards an equilibrium radius , while for $E_L > E_{L,c}$ an oscillating behaviour of the bubble is observed. For the PAA sample with 70% water content, the value of $E_{L,c}$ is situated between 8.9 mJ (where no pressure pulse was generated during bubble collapse) and 10.12 mJ. An example of an overdamped behaviour of the bubble is shown in Figure 4 for the case of a PAA sample with 70% water content and a laser pulse energy $E_L = 1.05$ mJ. The first frame was taken 15 μs after the moment of optical breakdown and the frame interval is 20 μs. Also shown in this figure is the hydrophone signal which was recorded simultaneously with the images documented in the photographic record.

The shock wave emitted during optical breakdown is a consequence of the plasma relaxation. Recent numerical calculations [6] indicate that the maximum pressure inside a bubble generated by 6-ns laser pulse during the initial phase of expansion is of the order of 10^4 MPa. This value is much higher that the yield stress of the PAA samples so that the material failed out during optical breakdown. This prevents the generation of a strong restoring elastic force during the initial stage of bubble expansion which may dissipate a part of the initial energy deposited by the laser pulse. Since almost the same amount of energy is available for the generation of the shock wave during breakdown both in water and PAA samples, the shock amplitude is independent of the mechanical properties of the medium. This also explains why the same scaling law between amplitude of the shock wave emitted during breakdown and laser pulse energy applies in water and PAA samples. However, as the pressure inside the bubble decreases as a consequence of bubble expansion, the material as a whole acts again as an elastic solid with a reduced elastic modulus due to the irreversible

material failure. A part of the bubble energy is dissipated during the expansion phase leading to a reduction of the maxi/mal bubble size. Consequently, less energy is available for bubble collapse, the bubble content becomes less compressed than in the case of water, and the pressure amplitude of the shock wave emitted during bubble collapse is diminished or even suppressed. For very soft materials (corresponding to PAA samples with 95% water content), the bubble dynamics do not differ substantially from that in water and the scaling law between pressure amplitude and laser pulse energy is similar to that in water. For stiff media (corresponding to PAA samples with 80% water content or smaller), the energy loss during bubble expansion is so large that it may lead to an overdamped behaviour of the bubble. Obviously, the damping of bubble oscillation becomes more and more pronounced with decreasing the laser pulse energy resulting in a steeper slope of the $p_c(E_L)$ curve for the PAA sample with 80% water content in Figure 3.
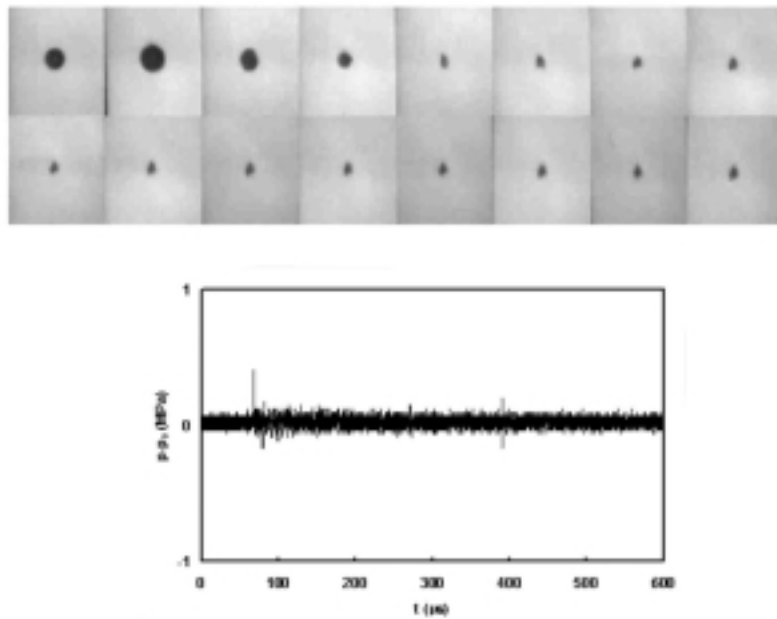
Figure 4. Cavitation bubble dynamics in the PAA sample with 70% water content (top) and the corresponding pressure signal measured at a distance of 10 mm from the laser focus (bottom) for a laser pulse energy $E_L = 1.05$ mJ. Frame interval 20 µs. Frame width 4 mm. The first pressure transient occurs during optical breakdown. The second pressure transient that occurs at a time $t = 390$ µs is the reflection of the pressure pulse emitted during optical from the free surface of the water.

4.   CONCLUSIONS

We found that, independent of the mechanical properties of the medium, the maximum pressure amplitude of the shock wave emitted during breakdown is proportional to the squared root of the laser pulse energy. In contrast, the maximum amplitude of the shock wave emitted during bubble collapse depends strongly on the properties of the medium surrounding the bubble. For soft media (corresponding to PAA samples with 95% water content), the pressure amplitude of the shock wave emitted during bubble collapse increases approximately proportional to the cube root of the laser pulse energy. For stiff media (corresponding to PAA samples with water content smaller than 80%), there is a critical value of the laser pulse energy below which the pressure pulse during bubble collapse is suppressed. Well above this value the scaling law is similar to that in water.

ACKNOWLEDGEMENTS

REFERENCES

1. JUHASZ, T., HU, X.N., TURI, L., BOR, Z., Dynamics of shock waves and cavitation bubbles generated by picosecond laser-pulses in corneal tissue and water, Lasers in Surgery and Medicine, **15**, pp. 91-98, 1994.
2. JANSEN, E.D., ASSHAUER, T., FRENZ, M., MOTAMEDI, M., DELACRETAZ, G., WELCH, A.J., Effect of pulse duration on bubble formation and laser-induced pressure waves during holmium laser ablation, Lasers in Surgery and Medicine, **18**, pp. 278-293, 1996.
3. ASSHAUER, T., DELACRETAZ, G., JANSEN, E.D., WELCH, A.J., FRENZ, M., Pulsed holmium laser ablation of tissue phantoms: correlation between bubble formation and acoustic transients, Applied Physics B, **65**, pp. 647-657, 1997.
4. DELACRETAZ, G., WALSH Jr., J.T., ASSHAUER, T., Dynamic polariscopic imaging of laser-induced strain in a tissue phantom, Applied Physics Letters, **70**, pp. 3510-, 1997.
5. VOGEL, A., CAPON, M.R.C., ASIYO-VOGEL, M.N., BIRNGRUBER, R., Intraocular photodisruption with picosecond and nanosecond laser-pulses - tissue effects in cornea, lens, and retina, Investigative Ophthalmology and Visual Sciences, **35**, pp. 3032-3044, 1994.
6. BRUJAN, E.A., Dynamics of shock waves and cavitation bubbles in bilinear elastic-plastic media, and the implications to short-pulsed laser surgery, European Physical Journal Applied Physics, **29**, pp. 115-123, 2005.
7. BRUJAN, E.A., NAHEN, K., SCHMIDT, P., VOGEL, A., Dynamics of laser-induced cavitation bubbles near an elastic boundary, Journal of Fluid Mechanics, **433**, pp. 251-281, 2001.
8. BRUJAN, E.A., NAHEN, K., SCHMIDT, P., VOGEL, A., Dynamics of laser-induced cavitation bubbles near elastic boundaries: Influence of the elastic modulus, Journal of Fluid Mechanics, **433**, pp. 283-314, 2001.
9. BRUNTON, J.H., High speed liquid impact, Philosophical Transactions of the Royal Society London A, **260**, pp. 79-85, 1966.
10. LESSER, M.B., FIELD, J.E., The impact of compressible liquids, Annual Review of Fluid Mechanics, **15**, pp. 97-122, 1983.
11. SCHOEFFMANN, H., SCHMIDT-KLOIBER, H., REICHEL, E., Time-resolved investigations of laser-induced shock-waves in water by use of polyvinylidenefluoride hydrophones, Journal of Applied Physics, **63**, pp. 46-51, 1987.
12. VOGEL, A., BUSCH, S., JUNGNICKEL, K., BIRNGRUBER, R., Mechanisms of intraocular photodisruption with picosecond and nanosecond laser-pulses, Lasers in Surgery and Medicine, **15**, pp. 32-43, 1994.